*29th EPS Conference on Plasma Phys. and Contr. Fusion Montreux, 17-21 June 2002 ECA Vol. **26B**, O-1.01 (2002)*

On the causality between transport reduction and induced electric fields in the edge of a tokamak

S. Jachmich, M. Van Schoor and R. Weynants

Laboratoire de Physique des Plasmas-Laboratorium voor Plasmafysica, Association 'Euratom-Belgian state', Ecole Royale Militaire- Koninklijke Militaire School, B-1000 Brussels, Belgium, Partner in the Trilateral Euregio Cluster

1. Introduction

Reducing the turbulent transport found in tokamaks is essential for achieving high confinement regimes. The plasma edge plays an important role in the physics of improved confinement. In this region, the shear in the $\boldsymbol{E}$x$\boldsymbol{B}$ velocity is responsible for the suppression of turbulence, but important neutral concentrations, steep gradients and the curvature of the geometry complicate its study. A consistent set of experiments and theory has been developed to analyse the important phenomena related to the formation of the electric field and the resulting reduction in radial transport. With the technique of electrode biasing and an adapted set of different probes and edge diagnostics we have been able to follow changes in the plasma flow, electric fields and density profiles. First we will discuss the temporal correlation in the regime of an oscillating electric field, where the onset and offset of transport barriers could be observed. The obtained hysteresis of sheared flow patterns and steep profile gradients confirm the mechanism of transport reduction caused by $\boldsymbol{E}$x$\boldsymbol{B}$ shear. Since in the examples reported here magnetic shear effects are not involved, we will take the shearing rate to be solely proportional to the electrical field gradient ∇E_r. Secondly we discuss the changes of the diffusion coefficient, which follow a form-factor that has been found to be common on various quantities. The last section deals with modelling of the electric field and the imposed rotation by taking into account our experimental findings on the effect of transport reduction.

Electrode biasing experiments are a standard scenario on Textor to study the H-mode [1,2]. The electrode voltage V_E is slowly ramped up to 600 V during the flat top phase of the discharge. The radial electric field follows the increasing voltage until a bifurcation occurs, where the electric field suddenly jumps to higher values. At the same time the electrode currents I_E drops, causing the power supply to oscillate (see Fig. 1a, red lines), and imposes rapid changes of the radial current j_r. The electric field, generated by j_r, not only sets-up a poloidal rotation, but also reduces the parallel viscosity, leading to a non-linearity in the radial conductivity. At a certain value of the electric field the viscosity is destroyed, the plasma spins-up and the bifurcation is triggered. Although at this time very high electric fields and shear rates are achieved, we like to point out that the transport and the confinement, represented by total number of confined electrons $N_{e,tot}$ and edge recycling H_α in Fig. 1b, are affected already prior the bifurcation. This is further supported by Fig. 2, where the normalised diffusion coefficient D is strongly reduced before the oscillations start. This observation is in agreement with a heuristic formula derived in [3], which describes the $D(\nabla E)$ dependence as follow:

$$D = D_{non} + D_{ano} \Big/ \left(1 + (\nabla E_r / \nabla E_{r,crit})^{\gamma}\right) \quad , \qquad (1)$$

with D_{non} describing the remaining transport and D_{ano} describing the suppressed transport. The exponent γ defines the rate of change for $\nabla E_r = \nabla E_{r,crit}$. Biglari *et al* [4] have found in case of strong shear γ=2/3 (BDT) , Shaing for weak shear γ=2 (SCH) [5] and Zhang *et al* for

arbitrary shear γ=2 (ZM) [6]. ∇E_{crit} is the critical electric field gradient, describing the efficiency of transport reduction, and is influenced by global parameters as demonstrated elsewhere [7].

2. Temporal correlation

The magnitude and location of the electric field gradient ∇E_r depend on the radial conductivity profile σ_r. As the electrode voltage V_E is increased, ∇E_r changes at the rate of the local σ_r (Fig. 3) until E_r is high enough to squeeze the banana orbits of the particles and to destroy the parallel viscosity (Fig. 3, "bifurcation"). This triggered, drastic decrease of σ_r causes ∇E_r to jump to much higher values. Since V_E is afterwards still increased, ∇E_r grows further, but at a smaller rate. Since the time scale of the orbit squeezing effect is very short no hysteresis between ∇E_r and V_E is visible during the voltage oscillations (see red curves). The edge transport, monitored by ∇n_e and H_α, and the core confinement, react to the oscillating voltage and the imposed ∇E_r changes, as shown by the obvious signatures in the time traces in Fig. 1b. The ∇E_r oscillates on the time scale of 1 ms, which is shorter than the typical particle confinement time. Since the turbulence needs to adjust, the effect on the particle transport and confinement is delayed and a hysteresis between D and ∇E_r develops (Fig. 2). As seen in Fig. 4 the electric field gradient is leading the formation of the transport barrier, represented by the density gradient at the same location, by about 5 ms. The time resolution of the electric field measurements is 40 μs and that of the edge density 2 ms. To corroborate our findings, the outermost interferometer channels, which has a time resolution of 200 μs, is displayed in Fig. 4. The delay in the density is ≈5.6 ms. Also note that the particle transport exhibits similar fine structures in time as ∇E_r does, which illustrates the firm link between D and ∇E_r.

3. Form-factor in suppressing turbulence

As Eq. (1) shows, already a modest amount of shear is sufficient to affect the transport. In fact the shear needed for the quenching of turbulence does not has to exceed a certain threshold. In [8] experimental results from fluctuation measurements have been presented, where also before the bifurcation lower fluctuation levels and partial decorrelation of turbulence have been clearly observed. The involved critical ***ExB*** shear can be determined by applying Eq. (1) to the data. The critical ***E***x***B*** shear corresponds to electric field gradient $\nabla E_{r,crit}$ for which the poloidal turbulence searing rate τ_s^{-1} is equal to the turbulence decorrelation rate τ_{co}^{-1} and is defined as $\nabla E_{r,crit} = \sqrt{2}\left(\left\langle k_\perp^2 \right\rangle D\right)_0 B_t$, whereby $\left(\left\langle k_\perp^2 \right\rangle D\right)_0$ characterises the turbulence in the absence of shear. The following scaling has been obtained (Fig. 5): $\nabla E_{r,crit} \propto B_t^{1.4} A^{-1.2}$, with B_t as the toroidal magnetic field and A as the atomic mass [7]. This scaling is also supported by other experiments, as indicated by the data of DIII-D and of CHS in Fig. 5. From gyro-kinetic simulations [9] a scaling $\nabla E_r \propto B_t^{1.3}$, which is very close to the Textor scaling. The fitted exponent γ in Eq. (1) is typically in the range of 2-4, which disagrees with the prediction by BDT , but is in line with ZM and SCH.

4. Edge modelling

The measurements are compared with the predictions of a one dimensional fluid model. In this model, parallel viscosity and neutral friction were already identified as important components to explain the very important and localised electric fields [10]. The continuity and moment equations are solved using the experimental temperature and ion density profiles as described in [11]. The neutral density is modelled as $n_0(r)=n_{0,a}\exp(-(r-a)/\lambda)$, with $n_{0,a}$ as the neutral density at the last closed flux surface (LCFS) and λ as the

decay length of the profile. In the computation $n_{0,a}$ and λ are adjusted so as to achieve the best agreement with the experimental profiles. The necessary values of these two quantities, as well as the global agreement between theory and experiment are a measure for the validity of the model. To see the effect when inertia (the anomalous effect is introduced via the radial velocity, modelled as V_r=-D_{ano} (∂n/∂r)/n) and shear viscosity (=mnD_{ano} $\partial V_\phi/\partial r$) is taken into account, the diffusion coefficient D_{ano} is varied from 0 to 1 m^2/s (Fig. 6), but kept constant along the minor radius r. Without any inertia and shear viscosity (D_{ano}=0m^2/s), λ has to be chosen of the order of a meter (which is unphysical) to avoid that the electric field becomes too large 1 cm inside the LCFS. This indicates that an additional damping mechanism should be included in the theory. When typical a value for D_{ano} of 1m^2/s is used, the computed E_r is much too small compared to the measured one. Even lowering the neutral density is not sufficient to reproduce the very localised and high electric field (green curve).

The only way to reproduce the observed electric field is to suppose that D_{ano} varies spatially as indicated by Eq. (1), with the experimentally determined $\nabla E_{r,crit}$ of 70 V/cm^2. The result can be seen in Fig. 7, where the blue curve, now including inertia and shear viscosity and taking into account the reduced transport, is in good agreement with the experimental E_r-profile. Furthermore we see that the decay length of the neutral density profile is of the order of a few cm now. Also for lower electric field profiles, measured before the bifurcation, better agreement with the computed ones has been found, when transport reduction due to $\boldsymbol{E}$x$\boldsymbol{B}$ shear is considered. It is interestingly to note that the modelled neutral density at the LCFS decreases, when E_r is increasing, which is confirmed by our experimental observation.

5. Conclusions

In polarisation experiments at TEXTOR two mechanisms are at work: one, essential for the built-up of E_r and rotation, and another one, for the resulting turbulence suppression. A non-linearity in σ_r causes an E_r-bifurcation and a spin-up of rotation. Since this occurs on a much shorter time scale than that of the quenching of turbulence, a hysteresis between the imposed shearing rate and the particle diffusion coefficient arises. This supports the hypothesis that the rotational shear is the responsible agent for turbulence suppression. The quantitative relation between D and ∇E_r has been confirmed also by other machines and modelling. Similar values for the critical $\boldsymbol{E}$x$\boldsymbol{B}$ shear have been determined. The measured $\nabla E_{r,crit}$ has been further used in our modelling. In the 1D-model inertia and shear viscosity terms have been considered to reproduced the measured E_r-profiles. However only when transport reduction due to $\boldsymbol{E}$x$\boldsymbol{B}$ shear is taken into account, the measured electric field profiles have been reproduced quite well. For these cases the computed neutral densities and decay lengths were in the expected range.

References

[1] R. Weynants *et al,Nucl. Fusion* **32** (1992), p. 837.
[2] S. Jachmich *et al,Plasm. Phys. Contr. Fus.* **40** (1998), p. 1105.
[3] G. Staebler *et al*, *Phys. Plasm.* **1** (1994), p. 909.
[4] H. Biglari *et al,Phys. Fluids B* **2** (1990), p. 1.
[5] K. Shaing *et al, Phys. Fluids B* **2** (1990), p. 1492.
[6] Y. Zhang *et al, Phys. Fluids B* **4** (1992), p. 1385.
[7] S. Jachmich *et al, Plasm. Phys. Contr. Fus.* **42** (2000), p. A147.
[8] J. Boedo *et al*, Proc. 18th IAEA Conf., Sorrento (2000), paper IAEA-CN-77/EXP5/22.
[9] C. Figarella *et al, submitted to Phys. Rev. Letters* (2002).
[10] J. Cornelis *et al, Nucl. Fusion* **34** (1994), p. 171.
[11] M. Van Schoor *et al*, *J. Nucl. Mat.* **290-293** (2001), p. 962; Proc. 15th PSI-conference, Gifu (2002).

Figures

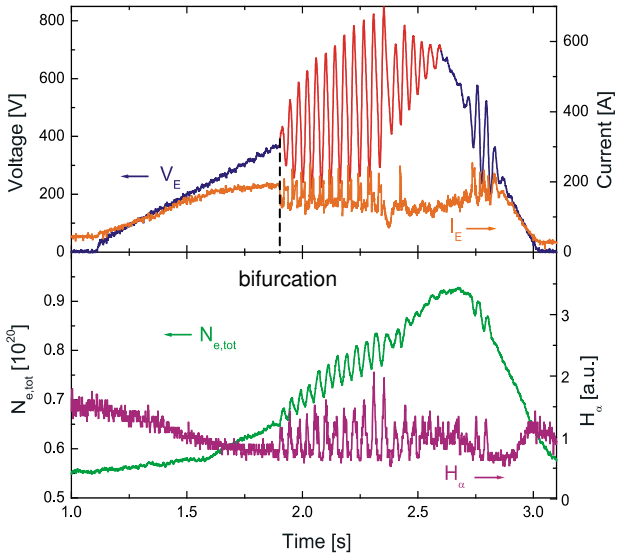

Fig 1: Time traces of electrode voltage V_E and current I_E, total number of confined electrons $N_{e,tot}$ and edge recycling H_α.

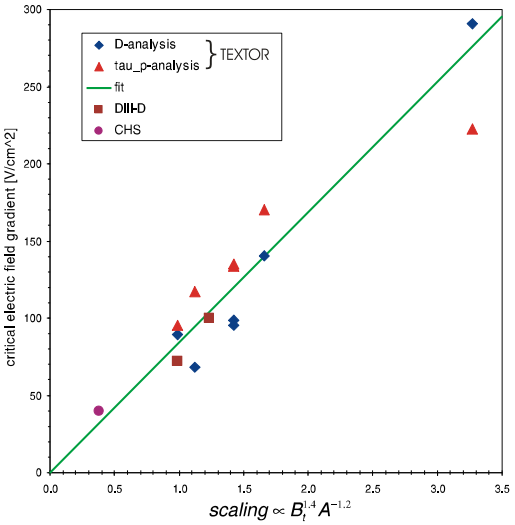

Fig. 5: Scaling of $\nabla E_{r,crit}$ with B and A

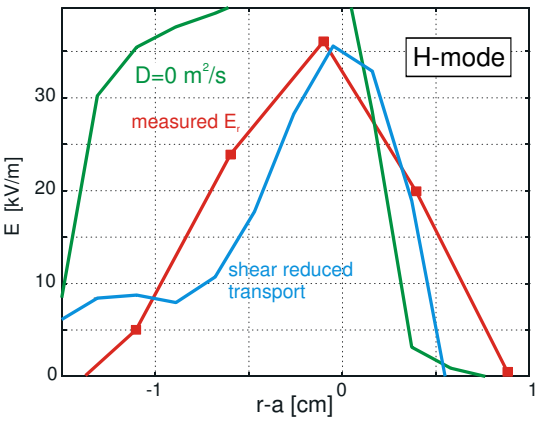

Fig. 7: E_r in H-mode w/o inertia and shear viscosity (D=0) and with shear reduction.

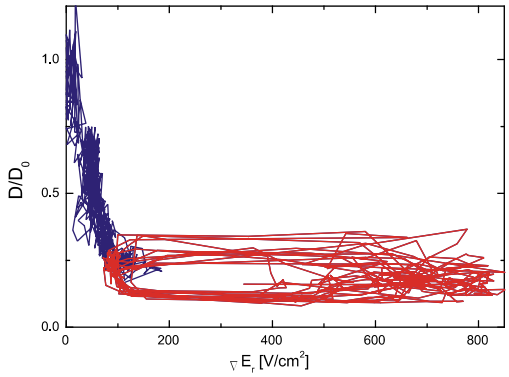

Fig. 2: Normalized diffusion coefficient vs. applied shear, represented by ∇E_r.

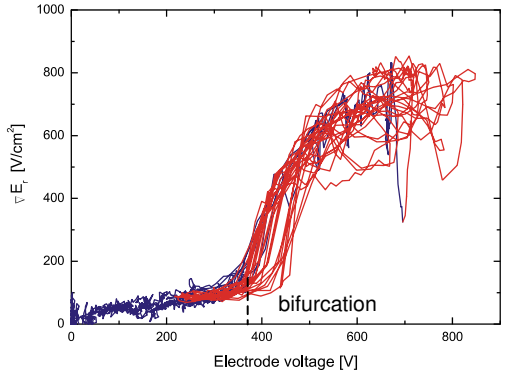

Fig. 3: Imposed electr. field gradient ∇E_r. vs. V_E.

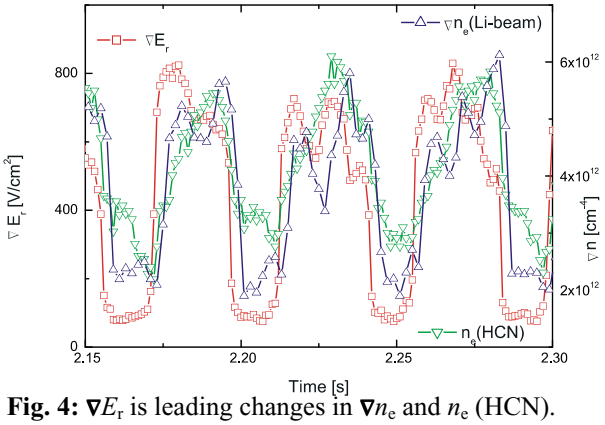

Fig. 4: ∇E_r is leading changes in ∇n_e and n_e (HCN).

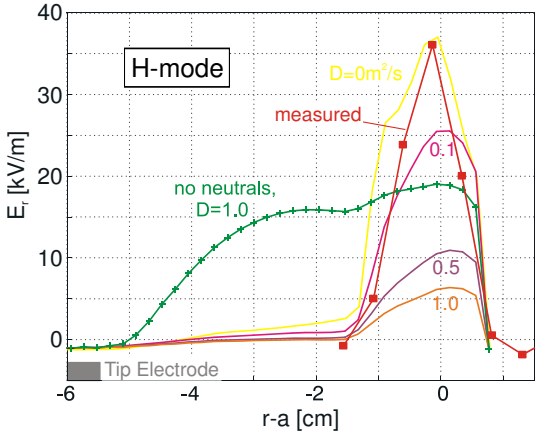

Fig. 6: E_r for several diffusion coefficients and for D=1 m/s^2 but with n_0 reduced by 100.